Physica B 724 (2026) 418187

Contents lists available at ScienceDirect

Physica B: Condensed Matter

journal homepage: www.elsevier.com/locate/physb

Boosting photocatalytic efficiency through Ni–Co co-doped ZnO thin films fabricated by spray pyrolysis

Ghada El Fidha [a], Nabila Bitri [a], Eduard Llobet [b,*]

[a] Laboratoire de Photovoltaïque et Matériaux Semi-Conducteurs, École Nationale d'Ingénieurs de Tunis, Université de Tunis el Manar, Tunis, 1002, Tunisia
[b] Microsystems Nanotechnologies for Chemical Analysis (MINOS), Universitat Rovira i Virgili, Avda. Països Catalans, 26, 43007, Tarragona, Spain

ARTICLE INFO

Keywords:
Ni–Co co-doped ZnO
Spray pyrolysis
Photocatalysis

ABSTRACT

Ni–Co co-doped ZnO thin films were synthesized on glass substrates via the spray pyrolysis technique to investigate the synergistic effect of dual doping on photocatalytic performance. The incorporation of Ni and Co ions effectively modified the structural, morphological, and optical properties of ZnO, as confirmed by XRD, SEM, AFM, EDX, and UV–vis spectroscopy. Photocatalytic tests under sunlight irradiation showed a remarkable enhancement in methylene blue degradation for Ni–Co co-doped ZnO films. In particular, 1.5 % Ni–Co co-doped ZnO achieves a 95 % degradation efficiency after 180 min of sunlight exposure.

1. Introduction

Metal oxide (MOX) semiconductor nanomaterials have attracted a great attention owing to their remarkable physical, chemical, optical and electronic properties. These characteristics make them suitable for a wide range of applications such as gas sensing, energy conversion, photocatalysis and optoelectronic devices [1–4]. The rising environmental impact of industrial effluents has recently increased the efforts to develop sustainable and effective wastewater treatment techniques. Conventional methods such as adsorption, coagulation, and biological degradation often fail to eliminate persistent organic pollutants or require complex and energy-intensive processes. In this context, advanced oxidation processes, particularly semiconductor-based photocatalysis, have appeared as promising alternatives due to their ability to mineralize toxic organic compounds into harmless by-products using sunlight energy [5,6].

Within this context, photocatalysis has demonstrated strong potential for the degradation of dyes, pharmaceuticals, pesticides, and other emerging contaminants in wastewater [6,7]. Recent research has highlighted the rapid development of metal-oxide-based photocatalysts capable of operating under solar irradiation, providing high degradation efficiency and stability [8,9]. Among them, metal oxides such as TiO_2, ZnO, and SnO_2 have been widely studied for water purification applications due to their stability, non-toxicity, and excellent chemical durability [10–12].

Zinc oxide (ZnO), in particular, has become a highly attractive candidate because of its wide band gap (3.37 eV), high exciton binding energy, low cost, and versatile nanostructures. Its favorable electrical and optical properties, combined with a high surface area, which are strongly dependent on the synthesis technique used, make of ZnO a suitable photocatalyst for solar-driven environmental applications [13,14]. Nevertheless, pure ZnO suffers from limited visible-light absorption and fast electron–hole recombination, which significantly restrict its photocatalytic performance [15]. Consequently, numerous strategies have been explored to enhance its activity, including the formation heterojunctions with other metal oxides or its doping or co-doping with transition metals [16,17].

Doping ZnO with transition metal ions such as Ni, Co, Mn, or rare-earth elements has proven effective in introducing defect states, improving charge separation, and extending light absorption toward the visible region [18,19]. Recently, co-doping has attracted considerable interest, as the simultaneous incorporation of two dopants can produce synergistic effects not achievable through single doping. Several studies have reported that co-doped ZnO systems enhance photocatalytic efficiency by generating additional oxygen vacancies, modifying lattice strain, and altering optical transitions [20,21]. Despite these advancements, the simultaneous effect of Ni and Co co-doping on ZnO thin films remains insufficiently explored, particularly for films prepared through scalable deposition methods. In that sense, spray pyrolysis has emerged as a simple, cost-effective, and industrially scalable technique capable of producing uniform, porous, and adherent thin films suitable for photocatalytic applications [22]. Its ability to control the microstructure,

---

* Corresponding author.
E-mail address: eduard.llobet@urv.cat (E. Llobet).

https://doi.org/10.1016/j.physb.2025.418187
Received 27 October 2025; Received in revised form 9 December 2025; Accepted 15 December 2025

porosity, and thickness through deposition parameters makes it a powerful method for engineering high-performance ZnO-based photocatalysts.

Previous works have extensively reported on the individual effects of Ni or Co doping in ZnO thin films [23,24]. However, systematic studies on the synergistic influence of Ni–Co co-doping remain scarce. To the best of our knowledge, no previous study has systematically explored the structural, optical, and photocatalytic properties of Ni–Co co-doped ZnO thin films prepared by spray pyrolysis, and has not assessed how dual doping influence their performance under natural solar irradiation.

Therefore, the objective of this study is to elucidate how Ni–Co co-doping influences the crystallinity, surface morphology, and band-gap energy of ZnO thin films, and to determine how these modifications affect their photocatalytic activity toward the degradation of methylene blue (MB). By correlating the structural and optical properties with the degradation kinetics. According to our current understanding, Methylene Blue (MB) was selected as the model pollutant due to its widespread use in textile, paper, and pharmaceutical industries, its high chemical stability, and its resistance to biodegradation. MB poses environmental and health risks even at low concentrations, making it an ideal candidate to evaluate photocatalytic efficiency. Monitoring MB degradation over time allows for a quantitative assessment of photocatalyst performance under defined experimental conditions [25,26].

2. Material and methods

2.1. Preparation of the thin films

Before the spray deposition, the glass substrates underwent a careful cleaning procedure to remove any surface contaminants. This process involved sequential treatment with detergent, deionized water, acetone, and a mixture of 1/4 HNO_3 and 3/4 HCl. After cleaning, the substrates were dried in an oven at 120 °C to ensure the complete removal of residual moisture and impurities.

Then, pure and Ni–Co co-doped ZnO thin films, with a fixed nickel concentration of 1 at.% and cobalt concentration varying from 0.5 to 2 at.% in steps of 0.5 at.%, were deposited using the spray pyrolysis technique. The spray solution was prepared by dissolving zinc chloride ($ZnCl_2$) (99.9 %, Sigma-Aldrich), nickel chloride hexahydrate ($NiCl_2{\cdot}6H_2O$) (99.9 %, Sigma-Aldrich, and cobalt chloride ($CoCl_2{\cdot}6H_2O$) (99.9 %, Sigma-Aldrich) in 40 mL of distilled water. The solution was continuously stirred using a magnetic stirrer to ensure complete dissolution and homogeneity. Then, the solution was sprayed onto the cleaned substrates for 10 min at a flow rate of 4 mL/min, with compressed air serving as the carrying gas at 10 mL/min. The substrate temperature was maintained at 400 °C. The distance nozzle-to-substrate and the hot plate rotation speed were set at 20 cm and 10 rpm, respectively. All deposition parameters were carefully controlled to produce homogeneous, porous, and well-adhered thin films, which are crucial for improved photocatalytic performance.

In fact, the dopant concentrations were carefully selected based on previous studies, which demonstrated that low to moderate doping levels enhance the photocatalytic performance of ZnO while preserving its crystalline structure. For instance, A. K. Azfar et al. [27] reported that 1 % Ni doping achieved the highest methylene blue (MB) degradation efficiency, whereas higher Ni contents led to decreased activity due to increased charge carrier recombination. Similarly, Co doping beyond 2–5 % may result in the formation of secondary phases such as Co_3O_4, which can adversely affect the optical and structural properties of ZnO [28]. Therefore, the chosen doping range was optimized to balance **structural integrity** and **photocatalytic efficiency**.

2.2. Photocatalytic tests

The photocatalytic activity of pure and Ni–Co co-doped ZnO thin films [Ni: 1 at.%, Co: 0.5–2 at.%] was evaluated using methylene blue (MB) as a model organic pollutant. A 3 mg/L aqueous MB solution was prepared and stirred to ensure homogeneity. Undoped and co-doped ZnO films were placed separately into five glass vessels, each containing 30 mL of the dye solution. To achieve adsorption–desorption equilibrium between the films and MB molecules, the suspensions were magnetically stirred in the dark for 30 min.

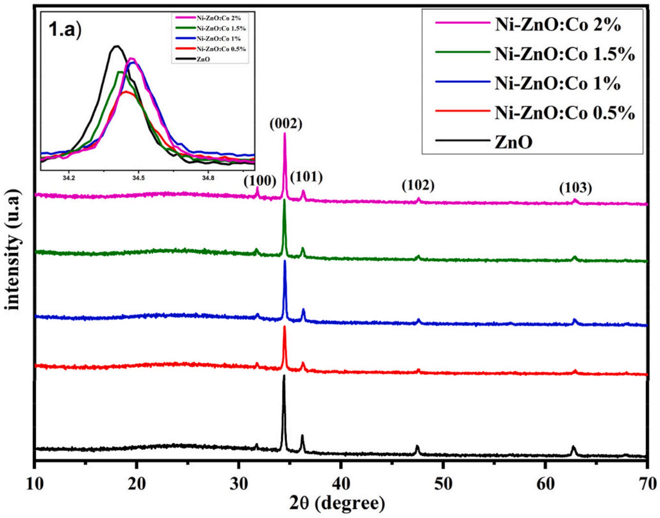

Fig. 1. X-ray diffraction spectra of ZnO thin films co-doped with Ni and Co. (a) Shifting of the main diffraction peak with increasing cobalt doping concentrations.

After equilibration, the samples were exposed to sunlight irradiation for a total duration of 3 h. Aliquots of 3 mL were withdrawn every 30 min for analysis. Photocatalytic experiments were carried out in Tunis, Tunisia irradiation (ambient temperature ≈ 38 °C, latitude 11.24°) under direct sunlight irradiation, with the MB photodegradation occurring at an estimated solar irradiance ranging from 180 to 230 W m^{-2}. The degradation of MB was monitored using a Shimadzu UV-1800 spectrophotometer, recording absorption spectra in the 450–900 nm wavelength range. A gradual decrease in the characteristic MB peak at 660 nm indicated progressive photocatalytic degradation.

2.3. Characterization of the thin films

The structural, optical, and morphological characteristics of the deposited ZnO thin films were systematically investigated to assess the impact of Ni–Co co-doping. X-ray diffraction (XRD) was employed to examine the crystal structure and confirm the incorporation of dopant ions. Optical properties were analysed using a Shimadzu UV-1800 spectrophotometer, providing insights into band gap modifications induced by co-doping. Morphological features were explored through field emission scanning electron microscopy (FE-SEM), revealing changes in surface topology associated with dopant incorporation. Additionally, atomic force microscopy (AFM, Dimension Icon, Bruker) in tapping mode was used to determine the root mean square (RMS) surface roughness, which is critical for understanding the photocatalyst–pollutant interaction and the enhancement of photocatalytic efficiency.

3. Results and discussion

3.1. Structural analysis

The X-ray diffraction (XRD) patterns of Ni–Co co-doped ZnO thin films with varying Co concentrations (0.5–2 at.%) at a fixed Ni content (1 at.%) are presented in Fig. 1. The XRD results reveal diffraction peaks at 31.77°, 34.39°, 36.32°, 47.64°, and 62.90°, corresponding to the

Table 1
Comparison of the thin film parameters for the different co-doped samples.

Thin film	Pure ZnO	Ni-ZnO-Co 0.5 %	Ni-ZnO-Co 1 %	Ni-ZnO-Co 1.5 %	Ni-ZnO-Co 2 %
Crystallite size (nm)	66	64	62.6	61	59
Dislocation density (δ) (10^{-4}) (nm^{-2})	2.29	2.44	2.55	2.68	2.87
Strain (ε) (10^{-2}) (rad)	4.18	4.15	4.4	4.85	4.56
Roughness (nm)	76	79	85	86.9	98.5
Thickness (nm)	300	320	365	400	420

(100), (002), (101), (102), and (103) planes of the hexagonal wurtzite structure of ZnO, respectively. Notably, the (002) plane exhibits the strongest intensity, indicating a preferential orientation along the c-axis. All observed peaks are in good agreement with the standard JCPDS card no. 01-080-0074. Importantly, no additional peaks corresponding to separate Ni or Co phases were detected, suggesting that Ni^{2+} ions are effectively substituted into Zn^{2+} lattice sites, while Co ions likely occupy interstitial positions, **demonstrating the successful incorporation of both dopants without forming secondary phases** [29]. As shown in Fig. 1a inset, the (002) peak gradually shifts towards higher 2θ angles with increasing Co concentration, which is due to the incorporation of Ni and Co ions into the ZnO crystal system. This behavior can be attributed to the substitution of Zn^{2+} ions (ionic radius 0.74 Å) by Ni^{2+} (0.69 Å) and Co^{2+} (0.72 Å) ions, which slightly alters the lattice structure and may influence the optical and photocatalytic properties of the co-doped ZnO thin films [30].

The crystallite size (D) of the ZnO thin films was estimated using the Debye–Scherrer equation [31]:

$$D = \frac{k\lambda}{\beta \cos \theta} \tag{1}$$

where k = 0.9, λ is a wavelength of 0.154 nm, β is full-width half maxima, and θ is the diffraction angle in radians.

The calculated crystallite sizes, summarized in Table 1, reveal a slight decrease in size upon Ni–Co co-doping. This reduction can be attributed to the substitution of Zn^{2+} ions by smaller Ni^{2+} and Co^{2+} ions within the ZnO lattice which induces distortions and defects into the ZnO lattice [32,33].

The dislocation density (δ) serves as a measure of the film crystalline quality, reflecting the extent of defects within the material [34]. δ is determined using equation (2) [35]:

$$\delta = \frac{1}{D^2} \tag{2}$$

As presented in Table 1, a slight increase in (δ) was observed with increasing dopant concentration, with the lowest value of 2.29×10^{-4} nm^{-2} obtained for the undoped ZnO thin film. This increase in dislocation density can be attributed to the incorporation of Ni and Co ions into the ZnO lattice. These distortions create additional strain within the crystal ZnO structure, which in turn leads to a higher density of dislocations.

The strain (ε), calculated using Equation (3) [35], is summarized in Table 1.

$$\varepsilon = \frac{\beta \cos \theta}{4} \tag{3}$$

A slight decrease in strain is observed with the addition of Ni and Co, reaching a minimum value of 4.15×10^{-2} rad for the 1 % doped film. However, as the Co concentration continues to increase, the strain begins to rise again, indicating a gradual build-up of lattice distortion at higher doping levels.

3.2. Morphological and compositional analysis

Atomic force microscopy was carried out to assess the surface topography of the films at different dopant concentrations. The three-dimensional AFM images (Fig. 2) reveal that the undoped and the Ni–Co co-doped ZnO at different dopant concentrations films exhibit a granular and compact morphology. The root-mean-square (RMS) roughness values were extracted using the WSxM 5.0 Develop 6.4

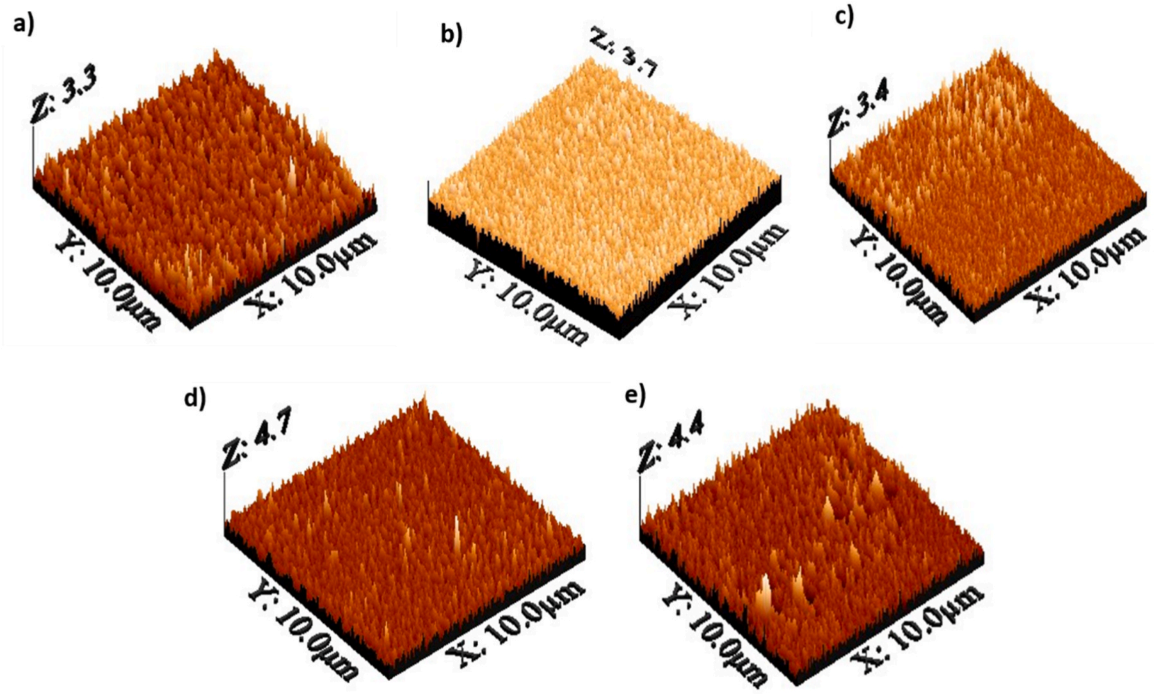

Fig. 2. Three-dimensional (3D) AFM topography for (a) undoped ZnO, (b) Ni-ZnO-Co 0.5 %, (c) Ni-ZnO:Co 1 % (d) Ni-ZnO-Co 1.5 % and (e) Ni-ZnO:Co 2 % thin films.

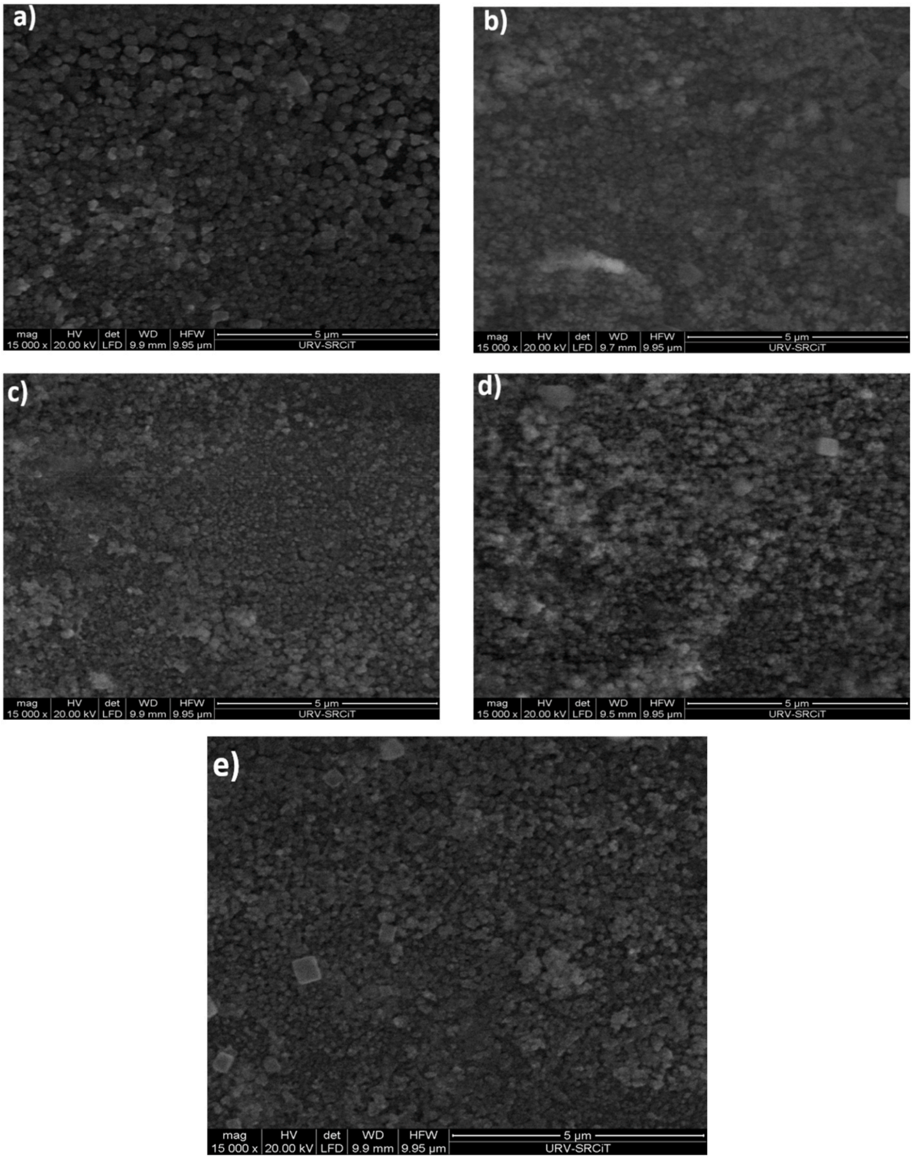

Fig. 3. SEM images of (a) pure ZnO, (b) Ni-ZnO-Co 0.5 %, (c) Ni-ZnO-Co 1 %, (d) Ni-ZnO-Co 1.5 % and (e) Ni-ZnO-Co 2 % thin film samples.

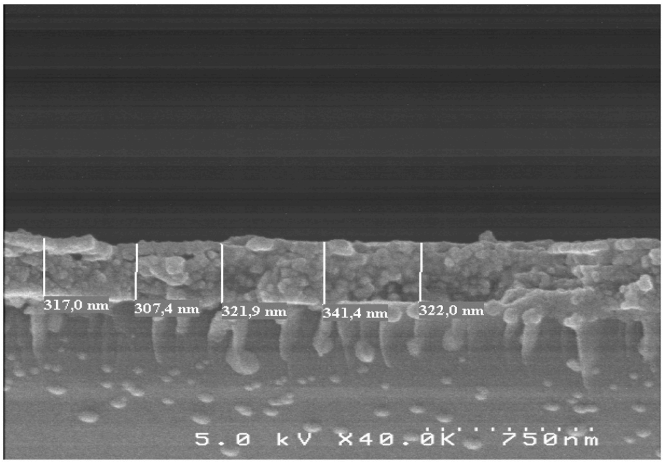

Fig. 4. Cross section of Ni-ZnO- Co 0.5 % thin film.

software. From the values presented in Table 1, a clear increase in roughness was observed upon doping. Indeed, the RMS roughness increases from 76 nm in undoped ZnO film to 98.5 nm for the sample doped with 2 % Co. In parallel, the surface texture became more irregular with a noticeable presence of agglomerations. These morphological changes are beneficial for the photocatalytic activity, as higher roughness and grain interconnection provide more active sites for dye adsorption and facilitate the degradation process [36].

The Field Emission Scanning Electron Microscopy (FESEM) images of Ni–Co co-doped ZnO thin films are presented in Fig. 3, revealing distinct structural features. The images show numerous microscopic grains aggregating to form a rough, granular surface with noticeable gaps and overlaps. A similar wrinkled, network-like morphology has been reported for ZnO thin films prepared via spray pyrolysis [37,38]. This network-like structure plays a crucial role in enhancing photocatalytic activity, as it provides a large number of active sites that facilitate surface reactions, thereby improving the photocatalytic efficiency [39].

The thickness of the thin films was estimated from the cross-sectional SEM images. Fig. 4 presents an example of the cross-section of an SEM image for a Ni- ZnO-Co 0.5 % thin film. These results are presented in Table 1. The value of the thickness of thin films for the undoped ZnO and

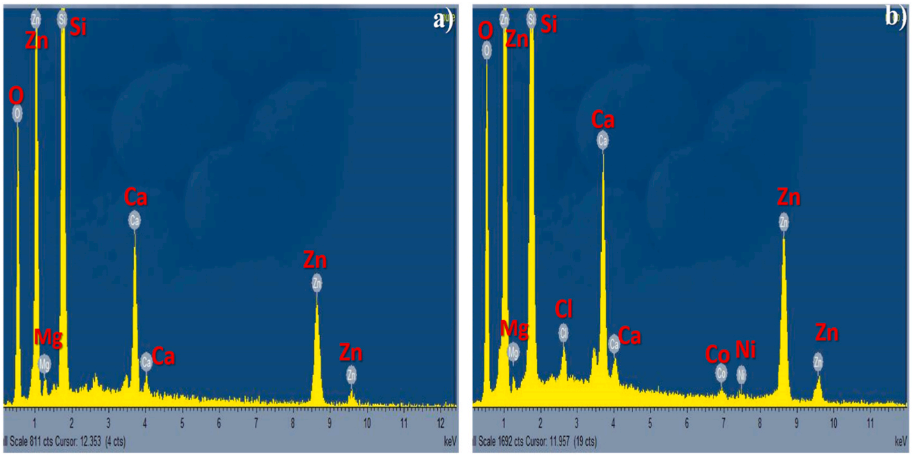

Fig. 5. EDX spectrum of the (a): undoped ZnO and (b): Ni ZnO-Co (1.5 %) thin films.

Table 2
Elemental concentrations calculated from EDS of ZnO thin films with different Ni and Co levels.

Thin film	Zn (at %)	O (at %)	Ni (at %)	Co (at %)	Si (at %)	Ca (at %)	Mg (at %)	Cl (at %)
Pure ZnO	19.53	56.26	0	0	18.39	4.48	1.34	–
Ni-ZnO-Co 0.5 %	20.76	54.13	0.78	0.28	17.48	5.20	0.83	0.41
Ni-ZnO-Co 1 %	19.39	53.06	0.69	0.61	19.22	5.56	0.96	0.54
Ni-ZnO-Co 1.5 %	20.28	54.38	0.7	0.86	17.65	4.32	0.91	0.89
Ni-ZnO-Co 2 %	17.57	55.10	0.61	1.02	19.26	4.65	0.84	0.95

for Ni and Co co-doped ZnO films range approximately from 300 to 420 nm. The increase in thickness with dopant concentration can be explained by the incorporation of foreign ions modify the growth kinetics of ZnO. Higher dopant levels increase the density of nucleation centers and enhance grain coalescence, which promotes a faster vertical growth rate of the film. These results are consistent with our AFM data, showing that the RMS roughness increases with dopant concentration, thus confirming that the enhanced dopant-induced grain growth allows the formation of thicker films. [18]. Indeed, the increase in film thickness may also contribute to the enhanced photocatalytic efficiency, as thicker films provide more active sites for dye adsorption and light absorption. These results are in agreement with recent studies on ZnO-based thin films [40].

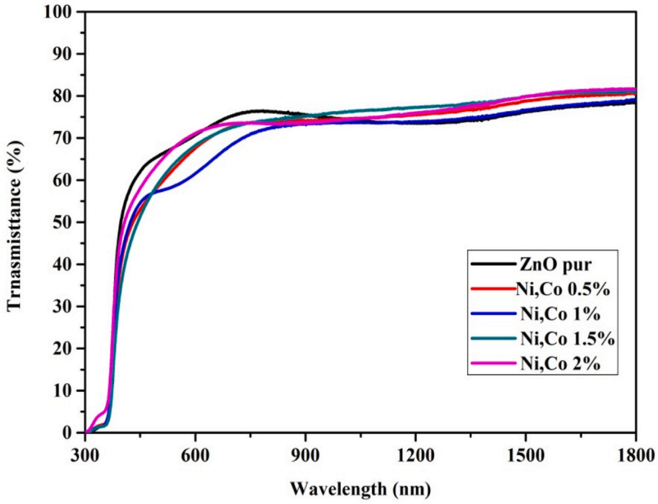

Fig. 6. Optical transmittance and reflectance spectra for the Ni,Co co-doped ZnO thin films.

The elemental composition of the Ni–Co co-doped ZnO thin films was analysed using Energy Dispersive X-ray (EDX) spectroscopy. The EDX spectra shown in Fig. 5, confirm the presence of Zn, O, Ni, and Co. The detection of Si, along with trace levels of Mg, Cl and Ca, is attributed to the composition of the glass substrate used for film deposition [12]. The elemental composition of the prepared thin films is summarized in Table 2. These results confirm the incorporation of Ni and Co into the ZnO lattice. The relatively high oxygen content observed in all samples can be attributed to the experimental conditions, particularly the use of distilled water (H_2O) as the solvent during the spray pyrolysis process.

These compositional results are consistent with the XRD analysis, which showed minimal peak shifts and slight changes in lattice parameters, further confirming the successful incorporation of the dopants into the ZnO crystal structure.

3.3. Optical analysis

The optical properties of the thin films were investigated using UV–vis absorption spectroscopy. The transmittance spectra of the pure and Ni–Co co doped ZnO thin films are shown in Fig. 6a. All films exhibit high transparency in the visible and near-infrared regions, with average transmittance values ranging from 75 % to 80 %. The remarkable transparency of these samples suggests their potential use for transparent conducting electrode applications [41].

A distinct absorption edge is observed in the UV region, which was analysed using Tauc's formalism [42].

$$(\alpha h\nu)^2 = A\left(h\nu - E_g\right) \tag{4}$$

$$\alpha = \frac{1}{d}\left(\frac{(1-R^2)}{T}\right) \tag{5}$$

where ν is the frequency of the incident photon, $h\nu$ is the photon energy,

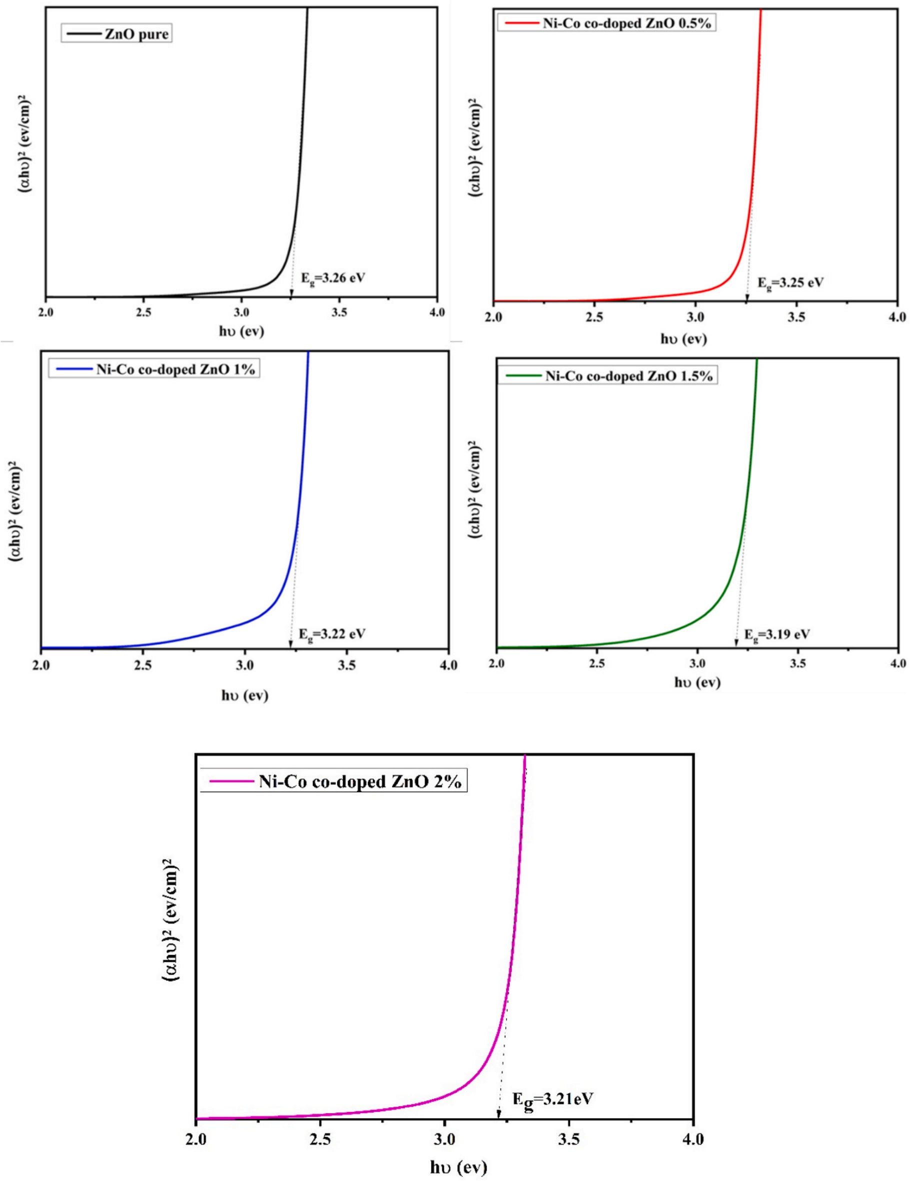

Fig. 7. Plot of $(ah\upsilon)^2$ versus (hυ) of undoped and Ni- Co-co-doped ZnO thin films at different doping concentration.

A is a constant (0.9) corresponding to the probability parameter for transitions, which reflects the degree of disorder in the material, and α is the absorption coefficient.

The optical band gap of ZnO thin films were measured for Ni and Co co-doped ZnO thin films at different doping concentrations (Fig. 7). Pure ZnO exhibits a band gap of approximately 3.26 eV, whereas increasing amounts of Ni and Co lead to a gradual reduction to 3.25 eV, 3.22 eV, and 3.19 eV for samples co-doped with Ni and Co at 0.5 %, 1 %, and 1.5 %, respectively. Interestingly, at the highest dopant level, the band gap slightly increases again to 3.21 eV. Indeed, the initial band gap narrowing is attributed to the introduction of structural disorder and defect states associated with the incorporation of Ni and Co, which introduce localized impurity levels within the forbidden gap [43].

Then, at the highest doping level (2 %), a mechanism that may contribute to the band gap widening is the saturation of defect states. As the dopant concentration increases to 2 % of Co, many of the defect-related states become fully occupied or compensated, which lowers the density of active sub-bandgap states. This saturation reduces sub-bandgap absorption, effectively increasing the band gap. As a result, fewer electronic transitions can occur at energies below the intrinsic band gap, leading to the observed blue shift. Similar behavior has been reported in other doped ZnO systems, supporting the role of defect state saturation in modifying the optical properties [44,45].

3.4. Photocatalytic activity

Photocatalytic degradation tests were conducted to assess the performance of pure ZnO and Ni–Co co-doped ZnO thin films in the removal of methylene blue (MB) under solar irradiation. The initial MB concentration was fixed at 3 mg L^{-1}. The degradation process was followed by measuring the evolution of the UV–vis absorbance spectra of the dye solution within the 450–900 nm range. As illustrated in Fig. 8, MB displays a prominent absorption peak at 660 nm, whose progressive decrease indicates the continuous degradation of the dye molecules during irradiation. The degradation efficiency, calculated using eq, (6), was evaluated for all samples after 180 min of exposure.

The photocatalytic degradation rate was calculated using the equation [46]:

$$\%\ \text{Photodegradation rate} = [(A_0 - A) / A_0] \times 100 \tag{6}$$

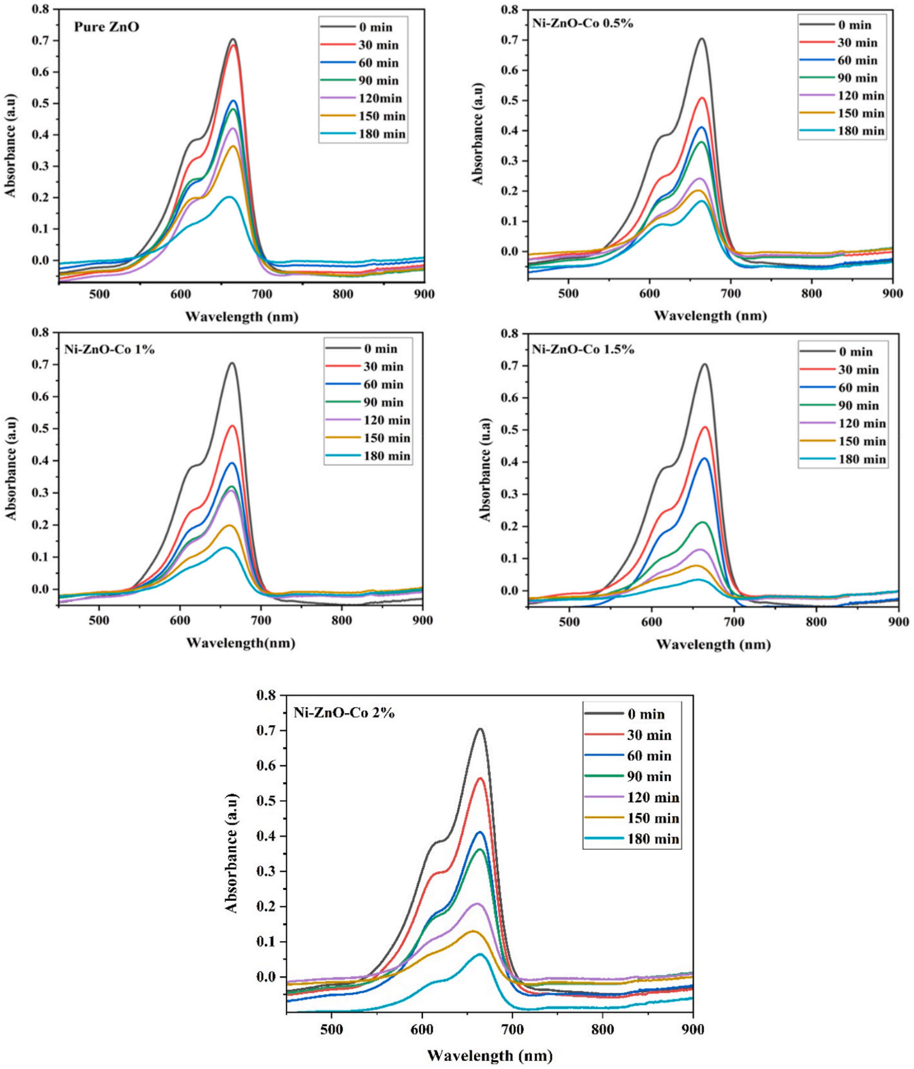

Fig. 8. Absorption spectra of MB after solar irradiation for 3 h using the Ni and Co co-doped ZnO thin films contents.

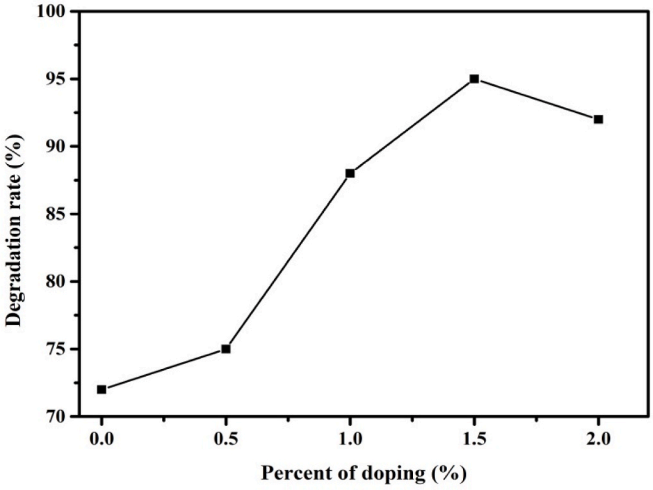

Fig. 9. Degradation rate of MB after solar irradiation for 3 h using the Ni-Co co-doped ZnO thin films at various Ni and Co contents.

where A_0 is initial absorbance of the dye solution and A is the absorbance after solar irradiation.

As shown in Fig. 9, pure ZnO achieved a degradation rate of 72 % after 180 min. Then, as the concentration of the dopant increases, the photocatalytic response increases as well. The highest activity observed was for the Ni and Co co-doped at 1.5 % film, which reached a degradation efficiency of 95 %. The efficiency of MB degradation exhibited a slight decrease for the sample doped at 2 % of Co.

This enhancement in the photocatalytic activity can be ascribed to the increased surface area, the creation of additional oxygen vacancies, and the inhibition of photogenerated electron–hole recombination induced by the incorporation of Ni^{2+} and Co^{2+} ions. Indeed, the presence of dopant ions allows electron–hole pairs to migrate to the surface, resulting in a higher generation of hydroxyl radicals [15,18,47]. Furthermore, the morphological and optical analyses affirm this improvement, showing that the ZnO sample co-doped at 1.5 % exhibits the lowest band gap energy and presents a high surface roughness (RMS), which promotes a higher adsorption capacity of MB molecules on the surface.

Table 3 present a comparison of the photocatalytic activities obtained for the different ZnO samples. Notably, the ZnO thin film co-doped with Ni and Co present the highest photocatalytic performance among all the samples studied. This performance is superior when compared to other reported studies on Ni and Co doped ZnO

Table 3
Comparison of photocatalytic activities of ZnO-doped and co-doped materials for degrading dyes.

Photocatalyst	Method of elaboration	Sources of Irradiation	Sources of Irradiation	Sources of Irradiation	Ref.
Ni-ZnO	Co-precipitation	visible light	Indigo carmine	91.67 %-150 min	[48]
Co-ZnO	Spray coating	UV irradiation	MB	76.31 % –120 min	[49]
Co-ZnO	Hydrothermal	artificial solar light	Rhodamine-B	64.13 %- 120 min	[50]
Cu- ZnO Ni	Spray pyrolysis	Sunlight	MB	92 %	[51]
Cu-Ni-ZnO	Co-precipitation	Visible light	Indigo carmine	93.32 %-60min	[52]
Ni-Eu-ZnO	Spray pyrolysis	UV lamp	Green malachite	93 % –120min	[53]
Ni-Co-ZnO	Co-precipitation	Visible light irradiation	RhB	42 % –360 min	[54]
Ni-ZnO-Co	Spray Pyrolysis	Solar irradiation	MB	95 % - 180min	This work

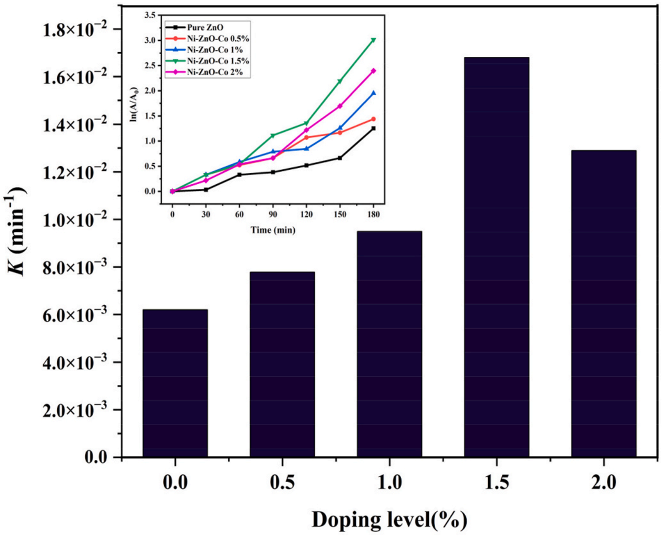

Fig. 10. The kinetic rate K as a function of Ni and Co content.

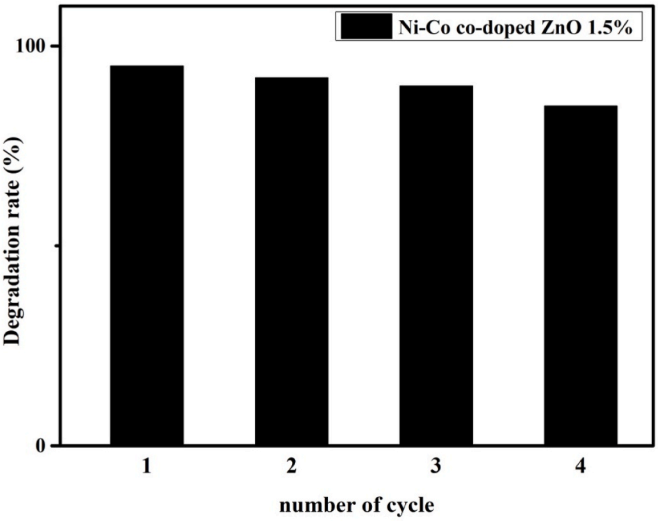

Fig. 11. Recyclability of Ni-ZnO co-doped Co at 1.5 %.

nanoparticles or other thin films co-doped with others materials, indicating that the optimized co-doping strategy significantly enhances the degradation efficiency.

3.4.1. *Photocatalytic kinetics*

The photocatalytic degradation of methylene blue (MB) by Ni–Co co-doped ZnO was investigated using a pseudo-first-order kinetic model, based on the Langmuir–Hinshelwood approach (equation (7)) [55]:

$$\ln\left(\frac{A_0}{A}\right) = Kt \tag{7}$$

where A_0 is the initial absorbance of the MB dye, A is the absorbance of MB dye after an irradiation time *t* and *K* is the pseudo first order rate constant. The constant rate *K* is calculated from the slope of the ln(A/A_0) versus the irradiation time *t* plot, and is shown in Fig. 10. The rate constant *K* increases with dopant concentration, reaching a maximum for the Ni-ZnO co-doped Co 1.5 % thin films and then decreases for the 2 % co-doped thin films. In fact, a higher rate constant indicates more efficient photocatalytic degradation. Nanostructure, surface defects, surface area, and reactivity all influence performance by enhancing electron transfer.

To evaluate the stability of the photocatalyst, four successive degradation cycles were carried out using the 1.5 % Ni–Co co-doped film (Fig. 11). Only a slight reduction in activity was observed after the fourth cycle, confirming the good stability and reusability of the material for solar-driven MB degradation. Overall, the enhanced photocatalytic performance originates from the combined effects of defect-induced charge separation, increased surface-active sites, and band-gap modulation induced by Ni–Co co-doping, demonstrating the potential of these thin films for environmental remediation applications [56].

3.4.2. *Mechanism of photocatalytic degradation*

Extensive research has been dedicated to clarifying the photocatalytic mechanism. This process consists of a series of oxidation and reduction reactions, in which electrons are excited from the valence band (VB) to the conduction band (CB), simultaneously producing oxidative holes (h^+) in the valence band and reductive electrons (e^-) in the conduction band [57,58]. These reactions are typically initiated when the energy of the incident light is equal to or exceeds the band gap energy of the catalyst (Fig. 12). Upon UV–visible light irradiation, Ni–Co co-doped ZnO nanoparticles absorb photons with energy equal to or greater than their band gap (Eg), generating electron-hole pairs (e^-/h^+).

$$ZnO + h\vartheta \rightarrow e_{CB}^{-} + h_{VB}^{+} \tag{8}$$

- e_{CB}^{+}: electron in the conduction band
- h_{VB}^{+}: hole in the valence band

Oxygen vacancies contribute to hole formation and enhance charge separation:

$$V_O^{+} + e^{-} \rightarrow V_O + h_{VB}^{+} \tag{9}$$

The photogenerated holes react with adsorbed water, producing hydroxyl radicals ($OH^{\cdot}$):

$$ZnO + h_{VB}^{+} + H_2O_{(ads)} \rightarrow H^{+} + OH^{\cdot} \tag{10}$$

Ni and Co dopants improve charge separation by trapping electrons in the conduction band, reducing recombination and enhancing radical formation:

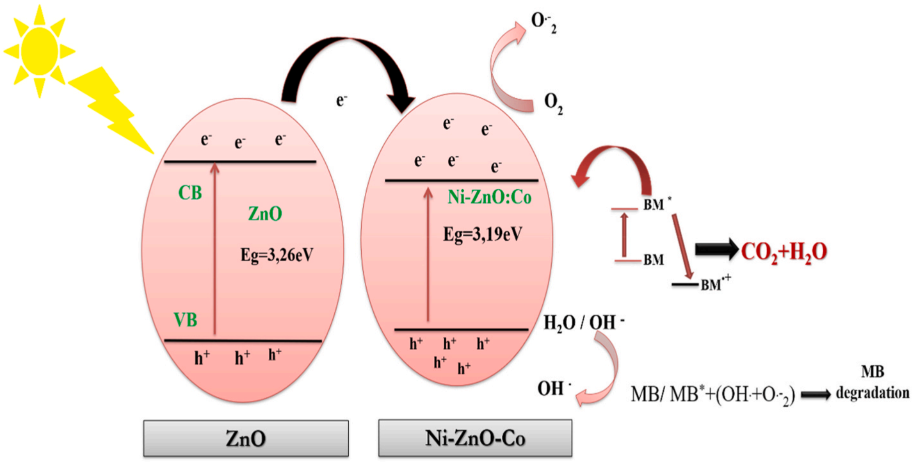

Fig. 12. Mechanism of photodegradation of MB by undoped ZnO and Ni and Co co-doped ZnO thin films under solar irradiation.

$$Ni^{2+} + Co^{2+} + e^{-}_{CB} \rightarrow Ni^{+} / Co^{+} \tag{11}$$

$$Ni^{+} / Co^{+} O_2(ads) \rightarrow O_2^{\cdot -} \tag{12}$$

$$O_2^{\cdot -} + H^{+} \rightarrow H_2O^{\cdot} \tag{13}$$

Water and oxygen molecules act as electron and hole scavengers, forming reactive radicals that attack methylene blue (MB):

$$H_2O^{\cdot} + H^{+} + e^{-}_{CB} \rightarrow H_2O_2 \tag{14}$$

$$H_2O_2 + e^{-}_{CB} \rightarrow HO^{\cdot} + OH^{-} \tag{15}$$

$$h^{+}_{VB} + H_2O \rightarrow H^{+} + OH^{\cdot} \tag{16}$$

$$H^{+} + OH^{\cdot} \rightarrow HO^{\cdot} \tag{17}$$

The hydroxyl radicals (OH·) generated in this process enable the degradation of MB molecules into CO_2 and H_2O:

$$MB_{dye} + HO^{\cdot} \rightarrow CO_2 \uparrow + H_2O \tag{18}$$

This mechanism, as schematically shown in Fig. 12, is explained by the Ni–Co co-doping of ZnO modifying its electronic structure, creating impurity levels that extend light absorption and enhance charge separation, thereby reducing electron-hole recombination. Consequently, the photocatalytic performance is markedly enhanced relative to that of pure ZnO.

4. Conclusion

In this work, undoped and Ni–Co co-doped ZnO thin films were successfully synthesized on glass substrates via the spray pyrolysis technique, offering a simple, cost-effective and scalable approach for thin film fabrication. Comprehensive characterization using XRD, SEM, AFM, EDX, and UV–vis spectroscopy revealed that Ni–Co co-doping effectively modulates the structural, morphological, and optical properties of ZnO films. The introduction of Ni and Co ions led to subtle band gap tuning, enhanced surface roughness, and increased density of active sites, all of which are critical factors for improving photocatalytic performance.

Photocatalytic tests using methylene blue as a model pollutant demonstrated a remarkable enhancement in degradation efficiency, with the 1.5 % Ni–Co co-doped ZnO film achieving the highest MB degradation activity of 95 % under sunlight irradiation. Moreover, the films exhibited excellent stability and reusability over multiple cycles, highlighting their potential for sustainable environmental remediation applications.

Overall, this study demonstrates that Ni–Co co-doping is a highly effective strategy to enhance the photocatalytic properties of ZnO thin films, providing new insights into defect engineering, charge carrier dynamics, and surface reactivity. These findings pave the way for the design of high-performance, solar-driven photocatalysts for practical wastewater treatment and other environmental applications.

CRediT authorship contribution statement

Ghada El Fidha: Writing – original draft, Visualization, Methodology, Investigation, Conceptualization. **Nabila Bitri:** Writing – review & editing, Validation, Data curation, Conceptualization. **Eduard Llobet:** Writing – review & editing, Resources.

Declaration of competing interest

The authors declare no conflicts of interest.

Acknowledgements

E. L. is supported by the Catalan Institution for Research and Advanced Studies (ICREA) via the 2023 Edition of the ICREA Academia Award.

Data availability

Data will be made available on request.

References

[1] Raghavendra Bairy Preethika, Anusha Dinakar Rao, Nayak N. Pawan, Suresh D. Kulkarni, Neelamma Gummagol, Laser-induced nonlinear optical tunability of Al-doped ZnO thin films for optoelectronic device applications, J. Alloys Compd. 1021 (2025) 179626.
[2] Anju Thomasa, Kalainathan Sivaperuman, Carbon and cobalt co-doped ZnO thin films for highly sensitive and selective ammonia detection at room temperature, Mater. Adv. 6 (2025) 629.
[3] R. Torkamani, B. Aslibeiki, Bulk ZnO, nanoparticles, nanorods and thin film: a comparative study of structural, optical and photocatalytic properties, J. Cryst. Growth 618 (2023) 127317.
[4] Xiangdong Meng, Guangye Fan, Luyao Xu, Binbing Zhang, Yinlong Chen, Yuxue Zhou, Feng Xu, Shaobo Zhang, Ag-induced surface significant enhanced luminescence of ZnO thin films prepared by sol-gel coating, Phys. B Condens. Matter 699 (2025) 416864.
[5] Tian-Hua Zheng, Zhen-Zhong Zhang, Yue Liu, Liang-Hua Zou Liang-Hua Zou, Recent progress in catalytically driven advanced oxidation processes for wastewater treatment, Catalysts 15 (8) (2025) 761.
[6] Surendar Balu, Dhanraj Ganapathy, Sandeep Ary, Raji Atchudan, Ashok K. Sundramoorthy, Advanced photocatalytic materials based degradation of micropollutants and their use in hydrogen production – a review, RSC Adv. 14 (2024) 14392–14424.

[7] Abdullah Al Miad, Shassatha Paul Saikat, Md. Kawcher Alam, Md. Sahadat Hossain, Newaz Mohammed Bahadur, Samina Ahmed, Metal oxide-based photocatalysts for the efficient degradation of organic pollutants for a sustainable environment: a review, Nanoscale Adv. 6 (2024) 4781–4803.

[8] Alishay Baig, Mohsin Siddique, andeep Panchal, A review of visible-light-active zinc oxide photocatalysts for environmental application, Catalysts 15 (2) (2025) 100.

[9] Sangram Keshari Sahu, Amrita Palai, Dojalisa Sahu, Photocatalytic applications of metal oxide-based nanocomposites for sustainable environmental remediation, Sustainable Chemistry for the Environment 8 (2024) 100162.

[10] S. Fatima, N. Abbas, J. Iqbal, M. Irshad, Ahazz Khan, Role and perspective of metal-oxide based nanocomposites for wastewater treatment: a review, Environmental Protection Research 4 (2) (2024) 128–155.

[11] Akshayakumar Kompa Sharanu, Anand Pal, Rao K. Mohan, Structural, spectroscopic, and electrical studies of spin-coated ZnO-ZTO thin films for their potential application in photocatalysis and optoelectronics, Ceram. Int. 49 (2023) 18272–18280.

[12] M. Mezyen, G. El Fidha, N. Bitri, aF. Harrathi, I. Lycand E. Llobet, Visible light activated SnO_2:Dy thin films for the photocatalytic degradation of methylene blue, RSC Adv. 13 (2023) 31151.

[13] Andriambahiny Ranto Ny Aina, Harry Patel, Subhajit Aich, Biplab Roy, Niladri Shekhar Samanta, Biswadeep Pal, Recent advances in ZnO based photocatalysts for industrial dye degradation, Discov. Appl. Sci. 7 (2025) 977.

[14] Souad Abou Zeid, Yamin Leprince-Wang, Yamin Leprince-Wang, Advancements in ZnO-Based photocatalysts for water treatment: a comprehensive review, Crystals 14 (7) (2024) 611.

[15] Frank Güell, Andrés Galdámez-Martínez, Paulina R. Martínez-Alanis, Ariadne C. Catto, Luís F. da Silva, Valmor R. Mastelaro, Guillermo Santana, Ateet Dutt, ZnO-based nanomaterials approach for photocatalytic and sensing applications: recent progress and trends, Mater. Adv. 4 (2023) 3685–3707.

[16] Buzuayehu Abebe, K. Neeraj, Gupta, Dereje Tsegaye, A critical mini-review on doping and heterojunction formation in ZnO-based catalysts, RSC Adv. 14 (2024) 17338–17349.

[17] Hafiza Mehwish Rasheed, Komal Aroosh, Depeng Meng, Xiaowen Ruan, Mansoor Akhter, Xiaoqiang Cui, A review on modified ZnO to address environmental challenges through photocatalysis: photodegradation of organic pollutants, Mater. Today Energy 48 (2025) 101774.

[18] G. EL Fidha, N. Bitri, F. Chaabouni, S. Acosta, F. Güell, C. Bittencourt, J. Casanova-Chafer, E. Llobet, Physical and photocatalytic properties of sprayed Dy doped ZnO thin films under sunlight irradiation for degrading methylene blue, RSC Adv. 11 (2021) 24917–24925.

[19] Buzuayehu Abebe, K. Neeraj, Gupta, Dereje Tsegaye, A critical mini-review on doping and heterojunction formation in ZnO-based catalysts, RSC Adv. 14 (2024) 17338–17349.

[20] Seniye Karakay, Leyla Kaba, Wrinkle type nanostructured of Al-Ce co-doped ZnO thin films for photocatalytic applications, Surf. Interfaces 44 (2024) 103655.

[21] Isa G.F. de Sá, Francisca P. Araújo, Francisco E. Paz dos Santos, Marcelo B. Furtini, Edson C. da Silva-Filho, Josy A. Osajima, Synthesis of ZnO co-doped with Er and co: effect of the dopants on the structural, optical properties and yellow eosin photocatalytic response, Solid State Sci. 147 (2024) 107400.

[22] Isa G.F. de Sá, Francisca P. Araújo, Francisco E. Paz dos Santos, Characterisation of porous doped ZnO thin films deposited by spray pyrolysis technique, Appl. Surf. Sci. 53 (2007) 9241–9247.

[23] Zhaoyu Luo, Ping Rong, Zhiyuan Yang, Jianhua Zhang, Xiangyu Zou, Qi YuPreparation and application of Co-Doped zinc oxide: a review, Molecules 29 (14) (2024) 3373.

[24] Ahmad Iqbal, Mehwish Aslam, Uzma Jabeen, Muhammad Nadeem Zafar, Muhammad Najam Khan Malghani, Norah Alwadai, Zahid Ullah, Ni-doped ZnO photocatalysts: synthesis, characterization and improved visible light driven photocatalytic degradation of methylene blue, Chimica Acta 543 (2022) 121167.

[25] T.A. Kurniawan, Z. Mengting, D. Fu, S.K. Yeap, M.H.D. Othman, R. Avtar, T. Ouyang, Functionalizing TiO_2 with graphene oxide for enhancing photocatalytic degradation of methylene blue (MB) in contaminated wastewater, J. Environ. Manag. 270 (2020) 110871.

[26] Yuliana de Jesús Acosta-Silva, Salvador Gallardo-Hernández, Sandra Rivas, Fabricio Espejel-Ayala, Arturo Méndez-López, Photocatalytic activities of methylene blue using ZrO_2 thin films at different annealing temperatures, Coatings 14 (2024) 537.

[27] A.K. Azfar, M.F. Kasim, I.M. Lokman, H.A. Rafaie, M.S. Mastuli, Comparative study on photocatalytic activity of transition metals (Ag and Ni)-doped ZnO nanomaterials synthesized via sol–gel method, R. Soc. Open Sci. 7 (2020) 191590.

[28] Buzuayehu Abebe, Bontu Kefale, Guta Amenu, Leta Guta, C.R. Ravikumar, Taymour A. Hamdalla, S. Giridhar Reddy, Dereje Tsegaye, H.C. Ananda Murthy, Cobalt-doped ZnO nanocomposits for efficient dye degradation: charge transfer, ChemistryOpen 13 (2024) e202400203.

[29] Noubeil Guermat, Warda Daranfed, Idris Bouchama, Nadir Bouarissa, Investigation of structural, morphological, optical and electrical properties of Co/Ni co-doped ZnO thin films, J. Mol. Struct. 1225 (2021) 129134.

[30] Akif Safeen, Kashif Safeen, Muhammad Shafiquea, Yousaf Iqbala, Sattam Al Otaibid, Ghafar Alie, Wiqar H. Shahf, Rajwali Khan, The effect of Mn and Co dual-doping on the structural, optical, dielectric and magnetic properties of ZnO nanostructures, RSC Adv. 12 (2022) 11923–11932.

[31] T.C. Paul, M.H. Babu, J. Podder, B.C. Dev, S.K. Sen, S. Islam, Influence of Fe^{3+} ions doping on TiO_2 thin films: defect generation, dd transition and band gap tuning for optoelectronic device applications, Phys. B Condens. Matter 604 (2021) 412618.

[32] Ahmed Johan Bashir, Md. Mintu Ali, Md. Jahidul Haque, Md. Humayan Kabir, Subhro Roy, Md. Shohan Ali, An approach to investigate the structural, morphological, and optical properties of spray pyrolyzed B and Mg co-doped ZnO thin films, Results Mater. 19 (2023) 100409.

[33] Neslihan Sakar, Zeynep Ertekin, Sibel Oguzlar, Mustafa Erol, La:ZnO nanoparticles: an investigation on structural, optical, and microwave properties, J. Mater. Sci. Mater. Electron. 35 (2024) 1355.

[34] M. Miki-Yoshida, J. Morales, J. Solis, Influence of Al, In, Cu, Fe and Sn dopants on the response of thin film ZnO gas sensor to ethanol vapour, Thin Solid Films 373 (2000) 137–140.

[35] I. Arora, et al., Structural, optical and electrical characterization of spin coated SnO_2: mn thin films, Mater. Today Proc. 36 (2021) 697–700.

[36] Nithyaa Sree Davamani, Stephen Rajkumar Inbanathan Savariroyan, The effect mo Mg on strucural and catalytic removal ol malachite green using ZnO thin films fabrication by cost effective home-made pyrolysis technique, Next Mater. 8 (2025) 10084.

[37] William Vallejo, Alvaro Cantillo, Carlos Díaz-Uribe, Improvement of the photocatalytic activity of ZnO thin films doped with manganese, Heliyon 9 (2023) 20809.

[38] F.A. Garcés, N. Budini, R.D. Arce, J.A. Schmidt, Thickness dependence of crystalline structure of Al-doped ZnO thin films deposited by spray pyrolysis, Procedia Mater. Sci. 9 (2015) 221–229.

[39] Faiqa Kanwal, Tariq Javed, Fayyaz Hussain, Muhammad Wasim, Maryam Batool, Enhanced dye photodegradation through ZnO and ZnO-based photocatalysts doped with selective transition metals: a review, Environmental Technology Reviews 13 (2024) 754–793.

[40] Alberto Bernal-Díaz, Agileo Hernández-Gordillo, Juan Carlos Alonso, Sandra E. Rodil, Monserrat Bizarro, Strong thickness dependence in thin film photocatalytic heterojunctions: the ZnO–Bi_2O_3 case study, Dalton Trans. 53 (2024) 7081–7092.

[41] F. Chaabouni, B. Khalfallah, M. Abaab, Doping Ga effect on ZnO radio frequency sputtered films from a powder target, Thin Solid Films 617 (2016) 95–102.

[42] J. Tauc, R. Grigorovici, A. Vancu, Optical properties and electronic structure of amorphous germanium, basic solid state physis 15 (1966) 627–637.

[43] S.J. Pearton, D.P. Norton, M. Ivill, A.F. Hebard, J.M. Zavada, ZnO doping strategies, J. Electron. Mater. 36 (2007) 462–471.

[44] M. Carofiglio, S. Barui, V. Cauda, M. Laurenti, Doped zinc oxide nanoparticles: synthesis, characterization and potential use in nanomedicine,m, Appl. Sci. 10 (15) (2020) 5194.

[45] W. Yang, B. Zhang, Q. Zhang, L. Wang, B. Song, Y. Ding, , et al.C.P. Wong, Structure and defects of ZnO quantum dots via tin doping, RSC Adv. 7 (2017) 11345–11354.

[46] R. Nasser, W.B.H. Othmen, H. Elhouichet, M. Férid, Preparation, characterization of Sb-doped ZnO nanocrystals and their excellent solar light driven photocatalytic activity, Appl. Surf. Sci. 39 (2017) 486–495.

[47] Madhurima Das, Avishek Ghatak, Preetam Guha Ray, Urszula Stachewicz, Advancements in ZnO-based photocatalysts for effective rhodamine dye removal from water, Sustain. Mater. Technol. 42 (2024) e01138.

[48] Rahul Kumar, R.S. Gedam, Enhanced photocatalytic activity of Ni doped ZnO nanoparticles for indigo carmine dye degradation, Materials Research Society Advances (2025), 01370-0.

[49] H. Sutanto, S. Wibowo, Hadiyanto, M. Arifin, E. Hidayanto, Photocatalytic activity of cobalt-doped zinc oxide thin film prepared using the spray coating technique, Mater. Res. Express 47 (2017) 076409.

[50] B. Poornaprakash, U. Chalapathi, K. Subramanyam, S.V.P. Vattikuti, S.H. Park, Wurtzite phase Co-doped ZnO nanorods: morphological, structural, optical, magnetic, and enhanced photocatalytic characteristics, Ceram. Int. 46 (2020) 2931–2939.

[51] Dilawar Ali, Raza Ali, Iqra Muneer, Rabia Ahson, Mohsin Ishtiaq, Muhammad Hammad Aziz, Rizwan Wahab, Spray pyrolysis grown Cu and Ni co-doped ZnO thin films: a study of their structural, optical, wettability, and photocatalytic performance, Physica Scripta 99 (2024) 1059c9.

[52] Rahul Kumar, R.S. Gedam, Synthesis and characterization of bi-functional Cu and Ni co-doped ZnO photocatalysts for organic pollutant degradation and antimicrobial activity, Ceram. Int. 50 (2024) 24716–24724.

[53] Beddiaf Zaidi, Moez Hajji, Mohammad Alam Saeed, Ghofrane Charrada, Bouzid Hadjoudja, Baghdadi Chouial, Najoua Kamoun-Turki, Synthesis, characterization, and photocatalytic performance of (Eu, Ni) Co-Doped ZnO thin films for environmental applications, J. Nano Res. 86 (2024) 77–88.

[54] P. Pascariu Dorneanu, I.V. Tudose, M. Suchea, Preparation and characterization of Ni, Co doped ZnO nanoparticles for photocatalytic applications, Appl. Surf. Sci. 448 (2018) 183–192.

[55] J.-C. Sin, S.-M. Lam, K.-T. Lee, A.R. Mohamed, Preparation of rare-earth-doped ZnO hierarchical micro/nanospheres and their enhanced photocatalytic activity under visible light irradiation, Ceram. Int. 40 (2014) 5431–5440.

[56] Mohammad Masuleh, Masood Hasheminiasari, Rouholah Ashiri, Enhanced photocatalytic efficiency of eco-friendly synthesized ZnO for rapid full degradation of methylene blue dye, Mater. Adv. 6 (2025) 2611–2621.

[57] Irshad Ahmad, R. Bousbih, Mahal Ahmed, Waheed Qamar Khan, Mohammed Aljohani, Mohammed A. Amin, Ali S. Alshomrany, Mohamed Shaban, Ijaz Ali, Hossein Bayahiya, Recent progress in ZnO-based heterostructured photocatalysts: a review, Mater. Sci. Semicond. Process. 180 (2024) 108578.

[58] Cabangani Donga, Rudzani Ratshiedana, Alex Tawanda Kuvarega, Ngonidzashe Masunga, Vijaya Srinivasu Vallabhapurapu, Pontsho Mbule, Photocatalytic degradation of organic pollutants in wastewater using magnetic

functionalized reduced graphene oxide nanocomposites. A review, Talanta 295 (2025) 128318.